Title

Composition Dependence of the Flory–Huggins Interaction Parameters of Block Copolymer Electrolytes and the Isotaksis Point

Journal

Macromolecules, 52(15)

ISSN

0024-9297

Authors

Loo, Whitney S
Sethi, Gurmukh K
Teran, Alexander A
et al.

Publication Date

2019-08-13

DOI

10.1021/acs.macromol.9b00884

Peer reviewed

Composition Dependence of the Flory-Huggins Interaction Parameters of Block Copolymer Electrolytes and the Isotaksis Point

Whitney S. Loo[†], Gurmukh K. Sethi[‡], Alexander A. Teran[†], Michael D. Galluzzo[†,▯], Jacqueline A. Maslyn[†,▯], Hee Jeung Oh[†], Katrina I. Mongcopa[†], Nitash P. Balsara[*,†,▯,§]

[†]Department of Chemical and Biomolecular Engineering, University of California Berkeley, Berkeley California 94720, United States

[‡]Department of Materials Science and Engineering, University of California Berkeley, Berkeley California 94720, United States

[▯]Materials Sciences Division, Lawrence Berkeley National Lab, Berkeley CA 94720

[§]Joint Center for Energy Storage Research, Lawrence Berkeley National Lab, Berkeley California 94720, United States

Correspondence to: Nitash P. Balsara (E-mail: *nbalsara@berkeley.edu*)

TOC Graphic

for Table of Contents use only

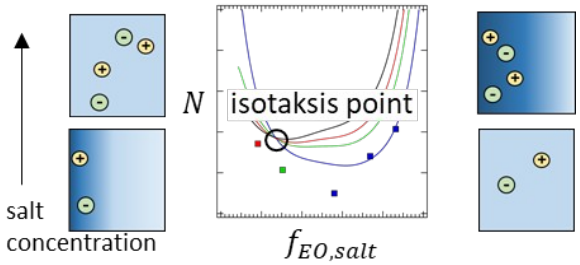

ABSTRACT

The thermodynamics of block copolymer/salt mixtures were quantified through the application of Leibler's Random Phase Approximation to disordered small angle X-ray scattering profiles. The experimental system comprises of polystyrene-*block*-poly(ethylene oxide) (SEO) mixed with lithium bis(trifluoromethanesulfonyl) imide salt (LiTFSI), SEO/LiTFSI. The Flory-Huggins interaction parameter determined from scattering experiments, χ_{SC}, was found to be a function of block copolymer composition, chain length, and temperature for both salt-free and salty systems. In the absence of salt, $\chi_{0,SC}$ is a linear function of $\left(Nf_{EO}\right)^{-1}$; in the presence of salt, a linear approximation is used to describe the effect of salt on $\chi_{eff,SC}$ for a given copolymer composition and chain length. The theory of Sanchez was used to determine χ_{eff} from $\chi_{eff,SC}$ in order to predict the boundary between order and disorder as a function of chain length, block copolymer composition, salt concentration, and temperature. At fixed temperature (100 °C), N_{crit}, the chain length of SEO at the order-disorder transition in SEO/LiTFSI mixtures, was predicted as a function of the volume fraction of the salt-containing poly(ethylene oxide)-rich microphase, $f_{EO,salt}$, and salt concentration. At $f_{EO,salt}>0.27$, the addition of salt stabilizes the ordered phase; at $f_{EO,salt}<0.27$, the addition of salt stabilizes the disordered phase. We propose a simple theoretical model to predict the block copolymer

composition at which phase behavior is independent of salt concentration ($f_{EO,salt}$=0.27). We refer to this composition as the “isotaksis point”.

INTRODUCTION

There is continued interest in understanding the thermodynamics of polymer/salt mixtures due to their applications as solid electrolytes in rechargeable batteries.[1–7] It is well known that the addition of salt to diblock copolymers greatly affects their thermodynamics and there have been many theoretical and experimental studies on quantifying these effects. A model system is polystyrene-*block*-poly(ethylene oxide) (SEO) mixed with lithium bis(trifluoromethanesulfonyl) imide salt (LiTFSI), SEO/LiTFSI. The transport of Li^+ ions in poly(ethylene oxide) (PEO) has been fully characterized[8] and the addition of polystyrene (PS) introduces mechanical support for the electrolyte.[9]

The phase behavior of pure diblock copolymers has been thoroughly studied, both experimentally and theoretically.[10,11] The equilibrium phase behavior is dictated by two parameters: the volume fraction of one polymer block, f_A, and the segregation strength, χN, where N is the overall degree of polymerization and χ is the Flory-Huggins interaction parameter, a measurement of the thermodynamic compatibility between the two polymer constituents. The temperature (T) dependence of χ is often given by

$$\chi = \frac{A}{T} + B \quad (1)$$

where A and B are empirically determined constants.[10,12] At high temperatures, entropy dominates leading to the formation of a disordered phase. As temperature decreases, the importance of the energy of

interactions between the two polymer blocks increases, and leads to microphase separation and the formation of ordered morphologies. For a given block copolymer, characterized by f_A and N, the transition from disorder-to-order occurs at a critical value of χ. Self-consistent field theory (SCFT) is a powerful tool that can predict the phase behavior of neat block copolymers.[13] At the order-disorder transition (ODT), the product χN may be given by

$$(\chi N)_{odt} = g(f_A) = C_0 + C_1(f_A - 0.5)^2 + C_2(f_A - 0.5)^4 + C_3(f_A - 0.5)^6 + C_4(f_A - 0.5)^8 \quad (2)$$

where the coefficients, C_i, are obtained by fitting Equation 2 to the SCFT results of Cochran et al.[11]: $C_0 = 10.5, C_1 = 47.9, C_2 = 782, C_3 = -3567$ and $C_4 = 24700$. In this theory, χ is an implicit property of the chemical structure of the constituent monomers in the block copolymer and does not depend on N or f_A. For a given block copolymer system at a particular temperature, T, Equation 2 can be used to calculate a critical chain length, N_{crit}, as a function of f_A:

$$N_{crit} = \frac{g(f_A)}{\chi(T)} \quad (3)$$

Block copolymers of a given composition, f_A, will be ordered if $N \geq N_{crit}$. A common way to measure χ is through the application of Leibler's Random Phase Approximation (RPA)[14], where small angle X-ray (SAXS) experiments can be used to measure concentration fluctuations by fitting the structure

factor, $S(q)$, to disordered scattering profiles. The interaction parameters derived from scattering are called χ_{SC}. There has been considerable debate about how the measured χ_{SC} relates to the value of χ that should be used in the SCFT calculations.[15–20] An attractive feature of N_{crit} is that it can be measured directly and interpreted without any debate.

The addition of salt is known to alter the thermodynamics of block copolymers due to the introduction of new interactions between the polymer chains and ions, e.g., electrostatic interactions, charge dissociation, ion solvation, ion translational entropy and physical cross-linking between the ions and polymer chains.[21–29] Ions tends to segregate in the phase with higher permittivity, which increases segregation strength between the salt-free and the salt-containing blocks. This was captured in models developed by Wang and coworkers using the concept of Born solvation energy.[30–33] In these models, χ is replaced with an effective interaction parameter, χ_{eff}, to account for the interactions introduced by salt. In the simplest case

$$\chi_{eff} = \chi_0 + mr \quad (4)$$

where χ_0 is the Flory-Huggins parameter for the salt-free system, r is a suitable measure of salt concentration and m is a system-dependent proportionality constant. This form for χ_{eff} in salty systems was first proposed in the pioneering work of Mayes and coworkers.[34]

In this paper, which builds on our previous study of the phase behavior of block copolymer electrolytes[35], we use the standard RPA-based analysis to determine the effective interaction parameter, $\chi_{eff,SC}$, from SAXS profiles of a series of disordered SEO/LiTFSI mixtures. Our experiments cover a wide range of block copolymer compositions, $0.18 \leq f_{EO} \leq 0.84$, and chain lengths, $49 \leq N \leq 414$. We also determine N_{crit} as a function of block copolymer composition. It is generally observed that adding salt stabilizes the ordered phase, i.e., m in Equation 4 is positive. This would imply that N_{crit} must decrease with added salt. We show that this is only true over a finite range of copolymer compositions, $0.27 \leq f_{EO} \leq 0.90$. In the range $0.15 \leq f_{EO} < 0.27$, N_{crit} increases with added salt and m is negative. We find that m is a smooth function of f_{EO}. For reasons that we clarify below, we propose using the term isotaksis composition to refer to the point where $m = 0$. For SEO/LiTFSI systems, the isotaksis composition is $f_{EO} = 0.27$.

EXPERIMENTAL SYSTEMS

Polymer Synthesis and Characterization

The polystyrene-*block*-poly(ethylene oxide) (SEO) copolymers in this study were synthesized via anionic living polymerization[36] and purified according to ref 37. The copolymers used in this study are called SEO(*xx*-*yy*), where *xx* and *yy* are the number-averaged molecular weights of the PS,

M_{PS}, and PEO, M_{PEO}, in kg mol^{-1}, respectively. Chain length, N, was calculated by $N = N_{PS} + N_{PEO}$ where

$$N_i = \frac{M_i}{\rho_i N_A \nu_{ref}} \quad (i = \text{PS or PEO}) \quad (5)$$

and N_A is Avogadro's number and ν_{ref} was fixed at 0.1 nm^3. The volume fractions of each block of the copolymers were calculated by

$$f_{EO} = \frac{\nu_{EO}}{\nu_{EO} + \frac{M_{PS} M_{EO}}{M_S M_{PEO}} \nu_S} \quad (6)$$

where ν_{EO} and ν_S are the molar volumes of ethylene oxide and styrene monomer units, respectively, and M_{EO} and M_S are the molar masses of ethylene oxide (44.05 g mol^{-1}) and styrene (104.15 g mol^{-1}), respectively. Molar volumes were calculated by $\nu = M/\rho$. In this study, the densities (g cm^{-3}) of the PEO and PS blocks were given by $\rho_{PEO} = 1.13$ and $\rho_{PS} = 1.05$, measured values at 90 °C. The neat copolymers are completely transparent and colorless. Table 1 gives the properties of the 8 SEO copolymers used in this study.

Table 1: Properties of copolymers in the study.

polymer	M_{PS}	M_{PEO}	N	f_{EO}
SEO(17.4-3.9)	17.4	3.9	342	0.18
SEO(9.4-	9.4	2.4	189	0.20

2.4)				
SEO(9.4-4.0)	9.4	4.0	214	0.29
SEO(1.7-1.4)	1.7	1.4	49	0.44
SEO(2.9-3.3)	2.9	3.3	99	0.52
SEO(3.8-8.2)	3.8	8.2	189	0.68
SEO(5.1-12.8)	5.1	12.8	281	0.71
SEO(4.0-22.4)	4.0	22.4	414	0.84

Electrolyte Preparation

The block copolymer electrolytes used in this study were prepared according to ref 38. The copolymers were dried at 90 °C under vacuum in a glovebox antechamber for at least 12 hours and then immediately brought into an argon environment. Lithium bis(trifluoromethanesulfonyl)imide (LiTFSI) salt (Novolyte) was transferred from its air-free packaging into a vial inside of a glovebox, and then dried at 120 °C under vacuum in a glovebox antechamber for three days. Due to the hydroscopic nature of the salt, Argon environment gloveboxes (Vacuum Atmosphere Company) with low oxygen and water levels were used for all sample preparation. The salt containing samples were prepared by blending SEO/benzene solutions with the required amount of a 75 wt% solution of LiTFSI/tetrahydrofuran (THF) solution to achieve the calculated salt concentrations.

For the salty samples, we assume that all of the salt resides in the PEO domain.[39–41] Block copolymers containing salt are considered to be pseudo-binary systems where the volume fraction of the salt + PEO component is given by

$$f_{EO,salt}=\frac{\nu_{EO,LiTFSI}(r)}{\nu_{EO,LiTFSI}(r)+\left(\frac{M_{PS}M_{EO}}{M_S M_{PEO}}\nu_S\right)} \quad (7)$$

where r is the molar ratio of Li to ethylene oxide (EO) moieties ($r=\frac{[Li]}{[EO]}$) and $\nu_{EO,LiTFSI}$ is the molar volume of the salt-containing PEO phase calculated by

$$\nu_{EO,LiTFSI}(r)=\frac{M_{EO}+r\,M_{LiTFSI}}{\rho_{EO,LiTFSI}} \quad (8)$$

where

$$\rho_{EO,LiTFSI}(r)=2.008r+1.13 \quad (9)$$

is derived from measured density values at 90 °C taken from ref 8.

Small Angle X-Ray Scattering (SAXS) Measurements

SAXS samples were prepared by pressing/melting the polymer into a 1/16 or 1/32 in. thick annular Viton rubber spacer (McMaster Carr) with an inner diameter of 1/8 in. at 120 ˚C in an argon glovebox and annealing at 120 ˚C for at least 12 hours under vacuum. The samples were cooled to room temperature under vacuum over the course of 24 hours. The samples were sealed with Kapton windows in custom-designed airtight Aluminum sample

holders. The samples were mounted in a custom-built 8-sample stage and annealed at each temperature for 20 minutes before performing measurements. SAXS measurements were conducted at the Advanced Light Source beamline 7.3.3 at Lawrence Berkeley National Lab[42] and Stanford Synchrotron Radiation Light Source beamline 1-5 at SLAC National Accelerator Laboratory. Scattering was performed using 10-12 keV X-rays.

Silver behenate was used to determine the beam center and sample-to-detector distance. The scattered intensity was corrected for beam transmission, empty cell scattering, as well as for unavoidable air gaps in the system. Glassy carbon (NIST) was used to determine the scaling calibration to obtain absolute intensity scattering. Two-dimensional scattering patterns were integrated azimuthally using the Nika program for IGOR Pro to produce one-dimensional (1D) scattering profiles.[43] In order to compare data collected at each beamline, temperature calibrations were conducted to measure the absolute temperature of the samples by making separate electrolyte samples with a thermocouple running through the sample holder. The data presented in the main text reflects the absolute temperatures of the samples.

EXPERIMENTAL RESULTS

Figure 1 shows the measured absolute scattering intensity (I) as a function of scattering vector, q, of the eight SEO copolymers in the salt-free

state at 90 °C. All eight copolymers are disordered, indicated by a single broad scattering peak, at all accessible temperatures. As the molecular weight of the copolymer increases, the location of the primary scattering peak, q^*, moves to a lower value of q, indicative of an increase in chain dimensions. However, the overall intensity of the scattering is not proportional to N. For example, SEO(4.0-22.4) has the lowest scattering intensity, but is the longest copolymer in the study.

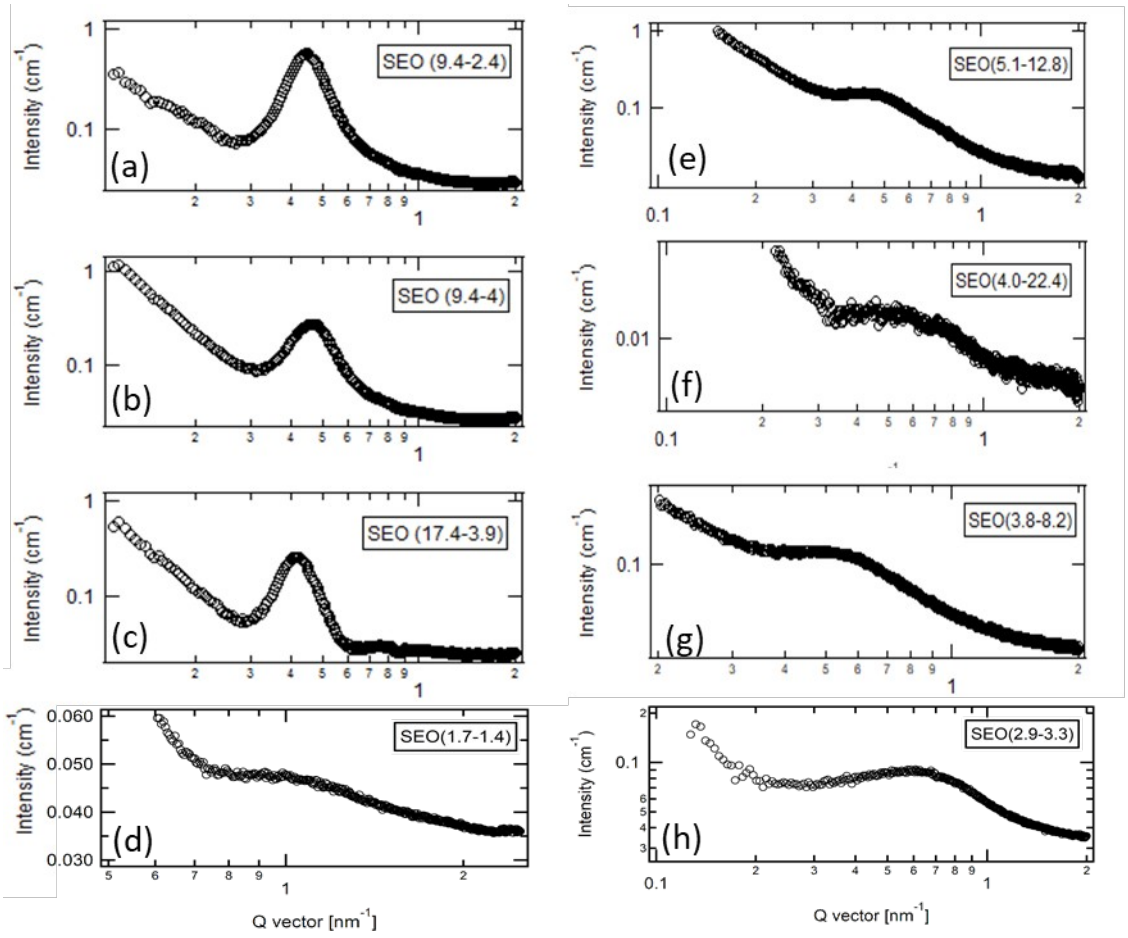

Figure 1: Absolute scattering for asymmetric copolymers in the neat state ($r=0$) at 90 °C for (a) SEO(9.4-2.4), (b) SEO(9.4-4.0), (c) SEO(17.4-3.9), (d) SEO(1.7-1.4), (e) SEO(5.1-12.8), (f) SEO(4.0-22.4), (g) SEO(3.8-8.2), and (h) SEO(2.9-3.3).

The scattering theory of monodisperse disordered diblock copolymers was developed by Leibler.[14] The scattering function $I(q)$ proposed by this theory for a perfectly monodisperse AB diblock copolymer with degree of polymerization N can be written as

$$I_{dis}(q)=C\left[\frac{S(q)}{W(q)}-2\chi\right]^{-1} \quad (10)$$

where C is the electron contrast calculated by

$$C=\nu_{ref}\left(B_A-B_B\right)^2 \quad (11)$$

where ν_{ref} is the reference volume, B_i is the X-ray scattering length density of block i given by $B_i=\frac{b_i}{\nu_i}$, and ν_i and b_i are the monomer volumes and X-ray scattering lengths of block i, respectively; $W(q)$ and $S(q)$ are the determinant and sum of the elements of the structure factor matrix $\left\|S_{ij}\right\|$. The expressions for $W(q)$ and $S(q)$ are given by

$$W(q)=S_{AA}^{\circ}S_{BB}^{\circ}-\left(S_{AB}^{\circ}\right)^2 \quad (12)$$

$$S(q)=S_{AA}^{\circ}+S_{BB}^{\circ}+2S_{AB}^{\circ} \quad (13)$$

where

$$S_{ii}^{\circ}=f_iN_i\nu_iP_i(q)\ (i=A,B) \quad (14)$$

$$S_{AB}^{\circ}=S_{BA}^{\circ}=\left(N_A f_A N_B f_B\right)^{\frac{1}{2}} F_A(q) F_B(q) \quad (15)$$

and

$$P_i(q)=2\left[\frac{\exp\left(-x_i\right)-1+x_i}{x_i^2}\right] \quad (16)$$

$$F_i=\frac{1-\exp\left(-x_i\right)}{x_i} \quad (17)$$

with $x_i=q^2 R_{g,i}^2$. Both blocks are modeled as flexible Gaussian chains and

$$R_{g,i}^2=\frac{N_i\left(\alpha a_i\right)^2}{6} \quad (i=PS, PEO) \quad (18)$$

where a_i is the statistical segment length of block i. In order to account for the conformational asymmetry between PS and PEO, we set a_{PS} = 0.50 nm and a_{PEO} = 0.72 nm (conformational asymmetry parameter, $\epsilon=\frac{a_{EO}}{a_S}=1.44$).[44–46] In Equation 18, a chain stretching parameter, α, is introduced to match experimental and theoretical values of $R_{g,i}$. N_i in Equations 14-18 is the number-average degree of polymerization for block i based on v_{ref}, and the calculated values are provided in Table 1. Equations 10-18 are used to analyze the scattering profiles from disordered block copolymer/salt mixtures. We ignore the fact that these equations were only developed for pure disordered block copolymers.[37,47–49]

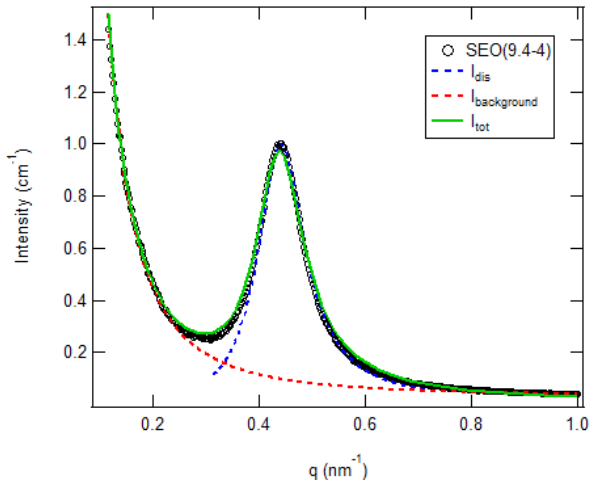

Figure 2: Example of RPA fit on neat SEO(9.4-4.0) at 75 °C. The open circles show the raw data and the green, blue, and red dashed curves show the fits for the total scattering, RPA fit, and background correction.

Figure 2 shows a typical SAXS profile obtained from salt-free SEO(9.4-4.0) at 75 °C. The open symbols show the data and the solid green line represents a fit to the equation

$$I_{tot}(q)=I_{dis}(q)+I_{bkgrd}(q) \quad (19)$$

where $I_{dis}(q)$ (shown in blue) is Equation 10 with χ, α and C as adjustable parameters and $I_{bkgrd}(q)$ (shown in red) is an exponential function to compensate for imperfect background subtraction. We find excellent agreement between the fitted function and the data.

We begin with a discussion of the fitted parameter, C. If we assume that the salt molecules remain strongly correlated with the EO segments in the disordered state, then we can consider our mixtures to comprise of two

"components": PS and PEO + salt. The density of homopolymer PEO/LiTFSI mixtures, $\rho_{EO,salt}$, as a function of r has been measured experimentally and is provided in Equation 9.[8] This can be used to calculate the theoretical scattering length density of these mixtures, $B_{EO,salt}$. If we assume that B_S is given by the known value obtained from homopolymer PS, then the only unknown in Equation 11 is $B_{EO,salt}$. The measurements of C thus provide a measurement of $B_{EO,salt}$, which we refer to as $B_{EO,salt}^{fit}$. This parameter can be used to calculate the effective density of the PEO/LiTFSI component, $\rho_{EO,salt}^{fit}$ using the following equations

$$\rho_{EO,salt}^{fit} = B_{EO,salt}^{fit}\left(\frac{\rho_{EO,salt}}{B_{EO,salt}}\right) \quad (20)$$

and

$$B_{EO,salt} = Y_{LiTFSI} B_{LiTFSI} + \left(1 - Y_{LiTFSI}\right) B_{EO} \quad (21)$$

where Y_{LiTFSI} is the volume fraction of LiTFSI in the PEO+salt phase calculated by

$$Y_{LiTFSI} = \frac{r\, v_{LiTFSI}}{(1+r)\, v_{EO,LiTFSI}} \quad (22)$$

where v_{LiTFSI} was calculated from ρ_{LiTFSI}=2.023 g cm^{-3}. These calculations were performed at 90 °C, the applicable temperature for Equation 9.

Figure 3a shows the averaged values of $\rho_{EO,salt}^{fit}$ for all eight copolymers as a function of salt concentration at 90 °C. The error bars represent the

standard deviation of the averaged data set. First, it is important to note that the individual values for $\rho_{EO,salt}^{fit}$ for all SEO copolymers collapse on to a single point for each salt concentration. This provides justification for our assumption that SEO/LiTFSI mixtures can be approximated as two-component systems. In other words, the change in density of PEO from homopolymer values is dependent only on salt concentration and not on copolymer properties, N and f_{EO}. The fitted density of PEO/LiTFSI is a weak function of salt concentration, decreasing by < 1% over the experimental salt concentration window (Figure 3a). This decrease is opposite to what has been observed in homopolymer PEO/LiTFSI mixtures.[8] Figure 3b is a plot of $\frac{\rho_{EO,salt}^{fit}}{\rho_{EO,salt}}$ versus salt concentration. The fitted density values are consistently lower than the homopolymer values. It is important to note that even in the absence of salt, $r=0$, $\frac{\rho_{EO,salt}^{fit}}{\rho_{EO,salt}}=0.95$ indicating that the density of PEO is affected by the presence of the PS block. The deviations between the fitted density and that of homopolymer/salt mixtures is less than 10% over the entire salt concentration window. These seemingly insignificant deviations in $\rho_{EO,salt}$ are important during the calculation of the scattering contrast because the electron density of the two phases (PS and PEO/LiTFSI) are

similar: a 7% decrease in $\rho_{EO,salt}$ results in a 100% increase in $\left(B_{EO,salt}-B_S\right)^2$ when $r=0.01$.

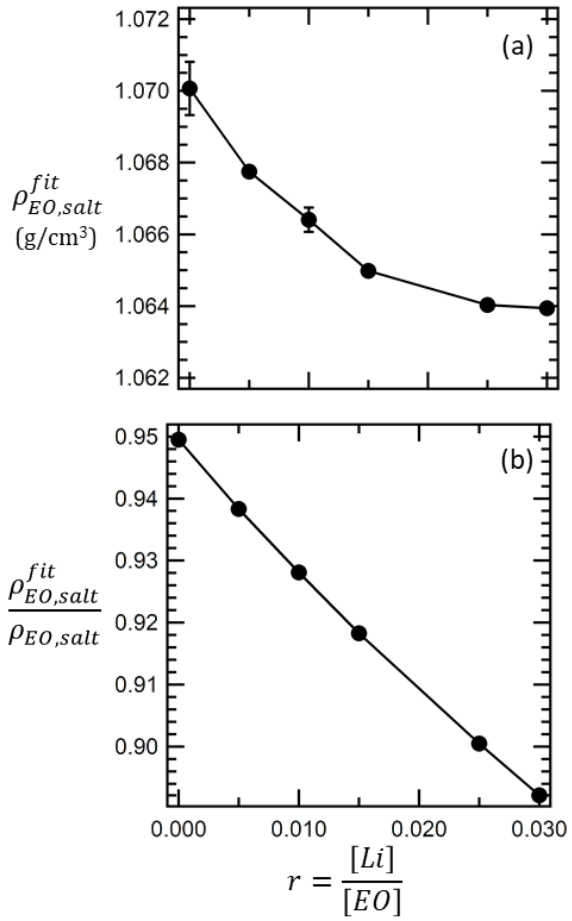

Figure 3: Results from fitting contrast during RPA fits: averaged values for (a) calculated salty PEO density, $\rho_{EO,salt}^{fit}$, and (b) ratio of fitted density to actual density, $\frac{\rho_{EO,salt}^{fit}}{\rho_{EO,salt}}$, as a function of salt concentration, r, taken at 90 °C. Error bars show the standard deviations for the data sets. Lines are used to guide the eye.

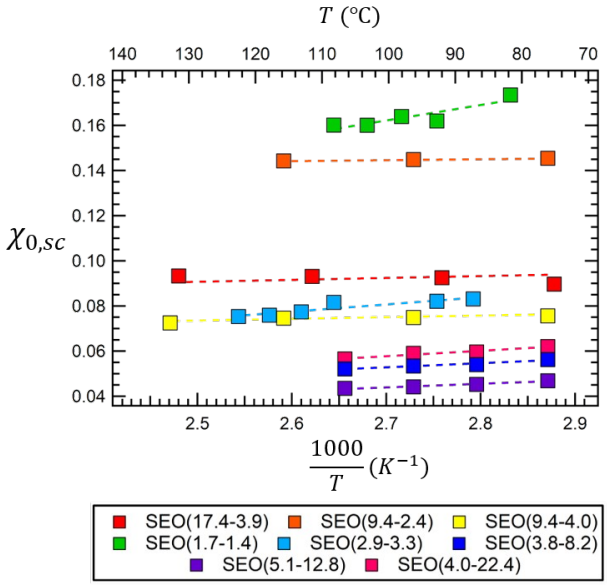

Figure 4: Temperature dependence for the Flory-Huggins interaction parameter for the neat SEO copolymers, $\chi_{0,SC}$. Dashed lines are fits to Equation 1.

The main parameter of interest is χ_{SC}, obtained by the fitting procedure depicted in Figure 2. Figure 4 shows the temperature dependence of $\chi_{0,SC}$,the Flory-Huggins interaction parameter determined from scattering for the salt-free block copolymers. The dashed lines are fits of the extracted $\chi_{0,SC}$ values presented in Figure 4 to Equation 1. The temperature dependence of $\chi_{0,SC}$ is consistent throughout the copolymers studied: $\chi_{0,SC}$ decreases with increasing temperature. However, the values of A and B obtained vary significantly between the copolymers. In other words, $\chi_{0,SC}$ depends on f_{EO} and N. There are no universally accepted functions for the dependence of $\chi_{0,SC}$ on composition and chain length. A simple function that is consistent with our data is shown in Figure 5 where we plot $\chi_{0,SC}$ obtained

at 100 °C versus $\left(f_{EO}N\right)^{-1}$. When data was not taken at exactly 100 °C, the fits to Equation 1 were used to interpolate $\chi_{0,SC}$ to 100 °C. The squares represent the data and the dashed line is a linear regression fit through the data,

$$\chi_{0,SC}=K_1+\frac{K_2}{Nf_{EO}} \quad (23)$$

The regression analysis gives $K_1=0.038$ and $K_2=2.85$.

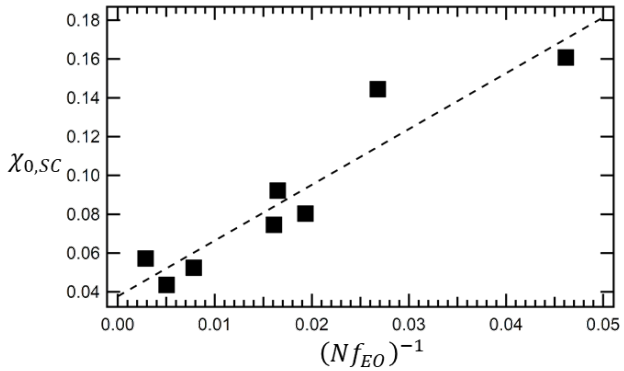

Figure 5: Chain length, N, and composition, f_{EO}, dependence on the Flory-Huggins interaction parameter of the neat copolymers, $\chi_{0,SC}$, at 100 °C. The dashed line is a linear regression through the data: $\chi_{0,SC}=\frac{2.85}{Nf_{EO}}+0.038$.

The functional form given in Equation 23 is motivated by the theory of Fredrickson and Helfand who theoretically examined the effect of concentration fluctuations on the phase behavior of block copolymers.[50] In this theory, the product χN at the ODT, $\left(\chi N\right)_{ODT}$, decreases with increasing N. For example, in symmetric systems with $f_A=0.50$, $\left(\chi N\right)_{ODT}=10.495+41.002N^{\frac{-1}{3}}$

. The mean-field value of $(\chi N)_{ODT}$ is only obtained in the limit of infinite chain length.[14] Equation 23 is similar in spirit and for finite f_{EO}, a composition- and chain-length-independent χ is obtained in the limit of infinite chain length. The product Nf_{EO} is equal to N_{EO}, the degree of polymerization of the PEO block. Equation 23 implies an implicit asymmetry in the thermodynamics between PS and PEO: a longer PEO block reduces the thermodynamic incompatibility between the two polymer blocks.

We now move to a discussion of the thermodynamics of the salt-containing SEO copolymers. Figure 6 shows the temperature dependence of $\chi_{eff,SC}$, the interaction parameter of the salt-containing species derived from scattering, for three SEO copolymers of similar chain lengths (N 200) with varying PEO compositions. Solid squares represent experimental measurements and the dashed lines are a fit through the data according to Equation 1. The temperature dependence of $\chi_{eff,SC}$ matches what was seen in the salt-free copolymers; A in Equation 1 remains positive. Figure 6a shows the temperature dependence of $\chi_{eff,SC}$ of SEO(9.4-2.4) with f_{EO}=0.20. As salt is added to the system, $\chi_{eff,SC}$ steadily decreases from 0.145 at r=0 to 0.140 at r=0.005 and finally to 0.13 at r=0.025 at 93 °C. In most cases reported in the literature, $\chi_{eff,SC}$ increases with increasing salt concentration.[51–55] Although the behavior of SEO(9.4-2.4) is unexpected, this trend has been previously reported in ref 37 for a SEO copolymer of a similar composition (SEO(1.9-0.8) with N=42 and f_{EO}=0.29). Figure 6b shows

the temperature dependence of $\chi_{eff,SC}$ of SEO(9.4-4.0) with f_{EO}=0.29. Here, we do not see a significant change in $\chi_{eff,SC}$ upon salt addition to r=0.005 indicating that at this copolymer composition, $\chi_{eff,SC}$ is not a strong function of r. Figure 6c shows the temperature dependence of $\chi_{eff,SC}$ of SEO(3.8-8.2) with f_{EO}=0.67. This copolymer shows a significant increase in $\chi_{eff,SC}$ upon salt addition (almost a 30% increase, from 0.50 at r=0 to 0.62 at r=0.005 at 100 °C). Figure 6 shows that the effect of salt addition on $\chi_{eff,SC}$ is highly dependent on copolymer composition.

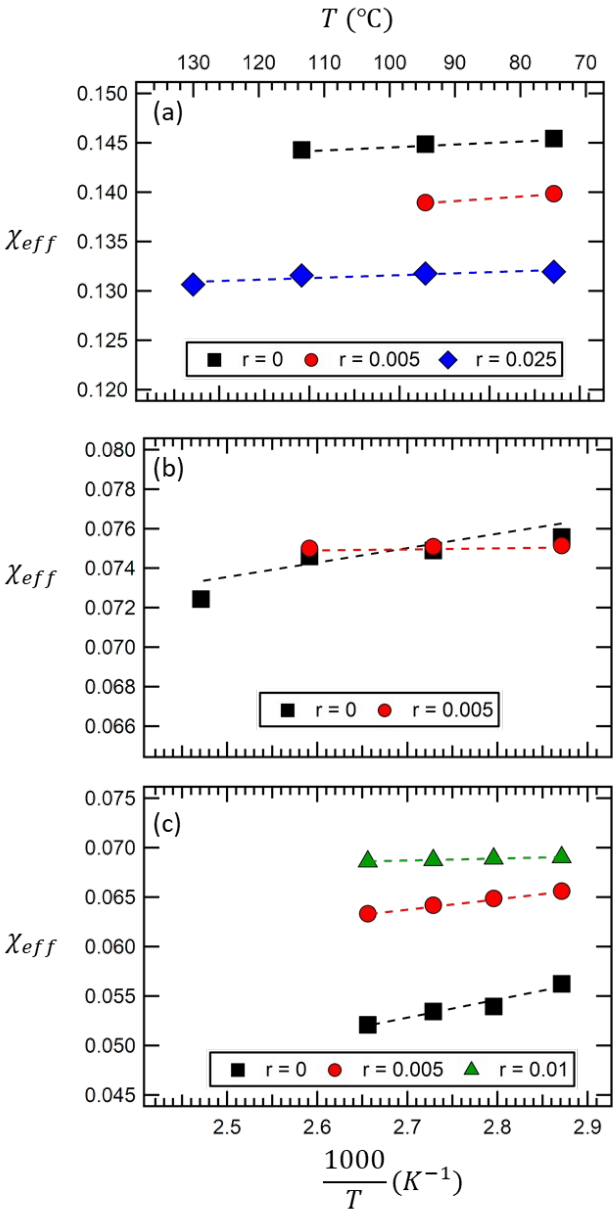

Figure 6: Temperature dependence of effective Flory-Huggins interaction parameter, $\chi_{eff,SC}$, for neat and salty samples of (a) SEO(9.4-2.4), (b) SEO(9.4-4.0), and (c) SEO(3.8-8.2). All copolymers have chain lengths around $N=200$. Symbols represent the data and dashed lines are fits to Equation 1.

Figure 7 shows the salt concentration dependence of $\chi_{eff,SC}$ for the eight SEO copolymers taken at 100 °C. Solid lines are used to connect the data points and serve to guide the eye. In general, $\chi_{eff,SC}$ increases with *r,*

except for SEO(9.4-2.4) as described above (shown in orange). For the low molecular weight SEO copolymers, SEO(1.7-1.4) (cyan) and SEO(2.9-3.3) (green), the effect of salt on $\chi_{eff,SC}$ seems to level-off at a given salt concentration as reported in ref 37, while for the copolymer with the highest PEO composition, SEO(4.0-22.4) (pink), $\chi_{eff,SC}$ increases linearly with salt concentration over the observed salt concentration window. It is obvious from Figure 7 that the effect of salt on $\chi_{eff,SC}$ is dependent on both N and f_{EO}.

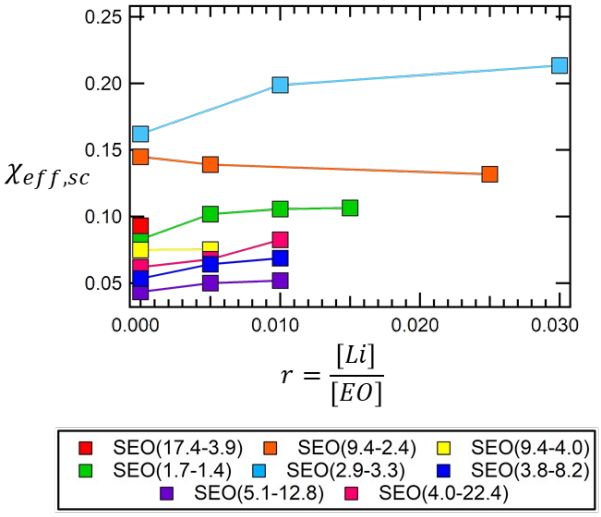

Figure 7: Salt concentration dependence for the effective Flory-Huggins interaction parameter, $\chi_{eff,SC}$, at 100 °C for the SEO/LiTFSI mixtures in the study. Lines are drawn to connect data points as a guide for the eye.

As a first approximation, each of the datasets presented in Figure 7 were fit to Equation 4, where m is a copolymer dependent proportionality constant. Figure 8 shows the composition dependence of m taken at 100 °C

weighted by the interaction parameters of the salt-free systems, $\chi_{0,SC}$. The dashed line is a linear regression through the data according to

$$\frac{m}{\chi_{0,SC}} = K_3 f_{EO} + K_4 \quad (24)$$

where $K_3 = 68.3$ and $K_4 = -18.6$. Note, only seven data points are presented in Figure 8 because there is no salt containing data for SEO(17.4-3.9), which orders immediately upon salt addition ($r \geq 0.005$). Equation 24 quantifies the dependence of rate of change in $\chi_{eff,SC}$ upon salt addition, given by m, on copolymer composition. We see excellent agreement between the data in Figure 8 and Equation 24. As the volume fraction of PEO increases, $\frac{m}{\chi_{0,SC}}$ increases. It is important to note that at the lowest value of f_{EO}, the ordinate of Figure 8 becomes negative, characterized by K_4.

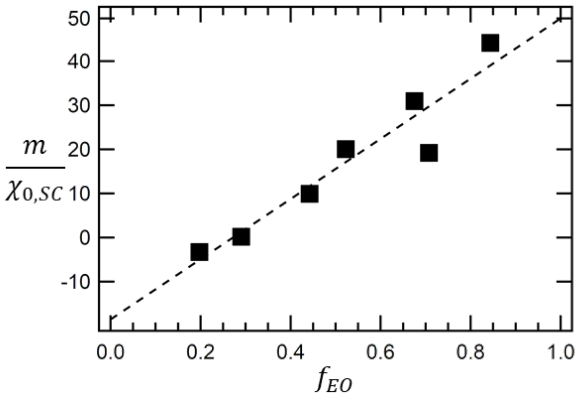

Figure 8: Composition, f_{EO}, dependence on the weighted slope of Equation 4, $\frac{m}{\chi_{0,SC}}$, taken at 100 °C. Dashed line is a fit to $\frac{m}{\chi_{0,SC}} = 68.2 f_{EO} - 18.6$.

Combining Equations 4, 23 and 24, we arrive at

$$\chi_{eff,SC} = \left[K_1 + \frac{K_2}{N f_{EO,salt}} \right] \left[1 + K_3 f_{EO,salt} r + K_4 r \right] \quad (25)$$

The comparison between Equation 25 and the data are presented in Figure 9 on a three-dimensional plot where $\chi_{eff,SC}$ is shown as a function of $f_{EO,salt}$ and r. The solid squares represent the extracted $\chi_{eff,SC}$ replicated from Figure 7, and the dashed lines represent fits to Equation 25 in the range of $0 \le r \le 0.03$. Overall, we see good agreement between the measured values of $\chi_{eff,SC}$ and Equation 25.

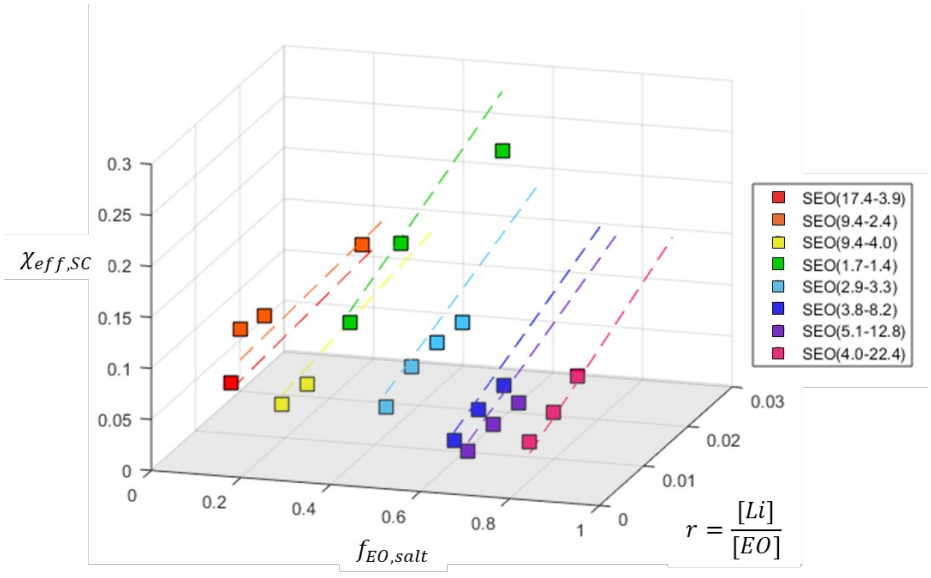

Figure 9: Model predictions for effective Flory-Huggins interaction, $\chi_{eff,SC}$, as a function of salt concentration taken at 100 °C. Dashed lines are the fits to Equation 25, $\chi_{eff,SC}=\left[K_1+\frac{K_2}{N f_{EO,salt}}\right]\left[1+K_3 f_{EO,salt} r+K_4 r\right]$. Data points are replicated from Figure 7. The slopes of the lines are negative for the block copolymers with $f_{EO,salt}<0.25$.

The final parameter extracted from the RPA fits is the chain-stretching parameter, α. In most cases, $\alpha>1$ implying that chains are stretched. In the neat copolymers, as temperature increases, α decreases (Figure SI1). At fixed tempeature, α for neat copolymers decreases with increasing f_{EO}. Figure SI2 shows data at 100 °C. At the highest f_{EO}, α is less than one. The addition of salt generally leads to an increase in α as shown in Figure SI3. The dependence of α on r, shown in Figure SI3, is very similar to the dependence of $\chi_{eff,SC}$ on r shown in Figure 7. In general, the increase in

effective repulsion between the blocks, quantified by $\chi_{eff,SC}$, leads to a larger value of α.

ORDER-DISORDER TRANSITION

The discussion thus far has focused on scattering from disordered SEO/LiTFSI mixtures. Whether or not a particular mixture is ordered depends on four variables: N, $f_{EO,salt}$, r, and T. Our discussion below is restricted to a fixed temperature of 100 °C. At fixed values of $f_{EO,salt}$ and r, one can, in principle, access a transition from disorder to order by increasing N. We define N_{crit} as the chain length at that transition. If χ is known, then Equation 3 can be used to determine N_{crit}.

As a first approximation, we assume that the Flory-Huggins interaction parameter extracted from scattering is equivalent to the theoretical parameter, $\chi_{eff,SC}=\chi$, and then use Equation 25 in conjunction with Equation 2 to calculate N_{crit}:

$$(\chi N)_{odt}=\left[K_1 N_{crit}+\frac{K_2}{f_{EO,salt}}\right]\left[1+K_3 f_{EO,salt} r+K_4 r\right]=g(f_{EO,salt}) \quad (26)$$

Equation 26 can be solved to obtain N_{crit} as a function of $f_{EO,salt}$ and r.

The solid curve in Figure 10a shows the calculated values of N_{crit} as a function of f_{EO} in the neat state, $r=0$. The model prediction is asymmetric with respect to copolymer composition, unlike predictions from mean-field

theory for conventional block copolymer systems[14], with a minimum at f_{EO}=0.37. The N_{crit} versus f_{EO} curve may be considered a phase boundary: systems below the curve are predicted to be disordered while those above the curve are predicted to be ordered. The squares in Figure 10a represent the SEO copolymers considered in this study, characterized by N and f_{EO}. All of the SEO copolymers are disordered in the neat state; however, several of the squares lie above the $N_{crit}(f_{EO})$ curve in Figure 10a. Therefore, it is evident that our assumption that $\chi_{SC}=\chi$ leads to an inconsistency in the model.

There are no published results for relating χ_{SC} to χ in block copolymers. However, for the case of polymer blends, Sanchez[15] presented a simple expression relating these two parameters by recognizing that :

$$\chi_{SC}=\frac{-1}{2}\left(\frac{\partial^2\left(f_A\left(1-f_A\right)\chi\right)}{\partial f_A^2}\right) \quad (27)$$

The solution for Equation 27, which first proposed by de Gennes[16], with appropriate boundary conditions is

$$\chi=\frac{2}{1-f_A}\int_0^{1-f_A}\left(1-f_A^{'}\right)\chi_{SC}\left(f_A^{'}\right)d\left(1-f_A^{'}\right)+\frac{2}{f_A}\int_0^{f_A}\left(f_A^{'}\right)\chi_{SC}\left(f_A^{'}\right)df_A^{'} \quad (28)$$

When Equation 25 for $\chi_{eff,SC}(f_{EO,salt})$is substituted into Equation 28 for $\chi_{SC}(f_A)$, we arrive at the following result

$$\chi_{eff} = \frac{\left(K_2 + K_1 N f_{EO,salt}\right)\left(1 - 2f_{EO} + 2f_{EO,salt}^2\right)\left(1 + K_3 f_{EO,salt} r + K_4 r\right)}{N f_{EO,salt}} \quad (29)$$

Equation 29 in conjunction with Equation 2 is used to calculate N_{crit}:

$$(\chi N)_{odt} = \frac{\left(K_2 + K_1 N_{crit} f_{EO,salt}\right)\left(1 - 2f_{EO} + 2f_{EO,salt}^2\right)\left(1 + K_3 f_{EO,salt} r + K_4 r\right)}{f_{EO,salt}} = g\left(f_{EO,salt}\right) \quad (30)$$

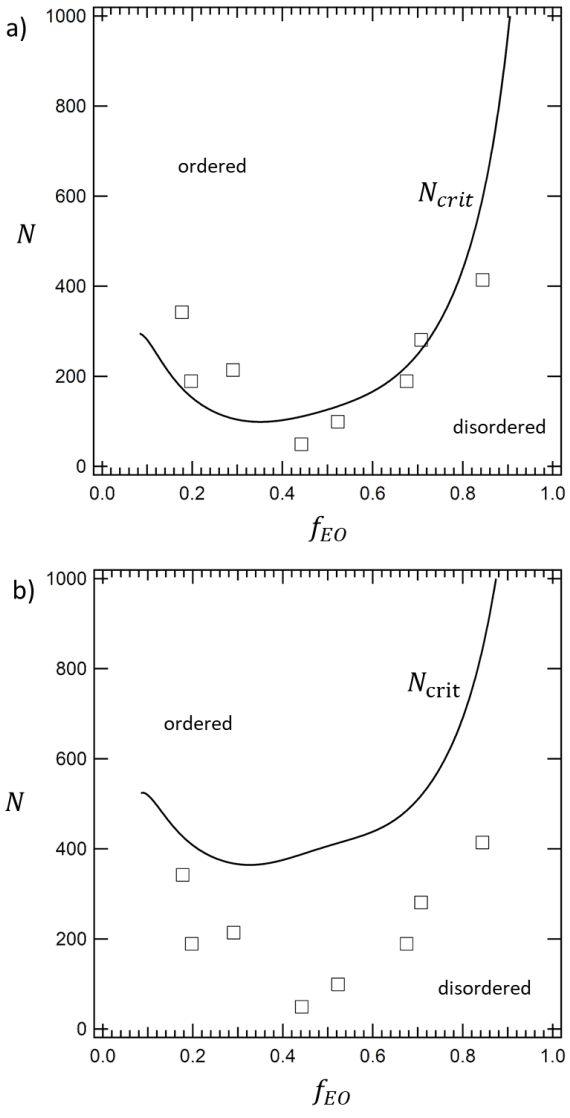

Figure 10: A plot of N versus f_{EO} for neat SEO copolymers ($r = 0$¿. The curve represents N_{crit} versus f_{EO} using a) Equation 25 or b) Equation 29 as χ_{eff}. Squares represent the values of N and f_{EO} of the SEO copolymers covered in this study. All of the copolymers are disordered in the neat state and thus we expect the data to lie below the N_{crit} versus f_{EO} curve. This is only the case when Equation 29 is used (b).

Equation 30 can be solved to obtain N_{crit} as a function of $f_{EO,salt}$ and r. Figure 10b shows the results of these calculations for the salt-free case. The predicted phase boundary remains asymmetric with respect to composition, but it moves to higher values of N_{crit} for all values of f_{EO} relative to Figure 10a. In Figure 10b, all of the data points lie underneath the $N_{crit}(f_{EO})$ curve indicating that all of the copolymers are predicted to be disordered in the absence of salt, consistent with our experiments. It is evident that accounting for the difference between $\chi_{eff,SC}$ and χ_{eff} is essential for quantifying the thermodynamic interactions in SEO/LiTFSI mixtures.

Based on the findings of Figure 10, we take Equation 29 to represent the Flory-Huggins interaction parameter in our system and use it to determine the effect of salt on critical chain length. The curves in Figure 11 show the composition dependence of N_{crit} for the salt concentrations of interest: r = 0 (black), r = 0.005 (red), r = 0.01 (green) and r = 0.025 (blue). The solid squares in Figure 11 represent the values of N and $f_{EO,salt}$ for the SEO/LiTFSI mixtures that order at $r \leq 0.025$. In these mixtures, the addition of salt leads to a transition from disorder to order. The color of each square in Figure 11 indicates the salt concentration at which the SEO/LiTFSI mixture

first forms an ordered morphology and matches the color of the N_{crit} curves. There is excellent quantitative agreement between theory and experiment on the high $f_{EO,salt}$ side. For $f_{EO,salt} \leq 0.58$, the experimental data lie well below the theoretical curves. There is, however, some correspondence between the theoretical curves and experimental data. The curve for r = 0.025 (blue) dips to the lowest value of N_{crit}, consistent with the data at $f_{EO,salt}=0.58$. At $f_{EO,salt}=0.29$, the curve for r = 0.01 (green) is above the r = 0.025 curve (blue), consistent with the data.

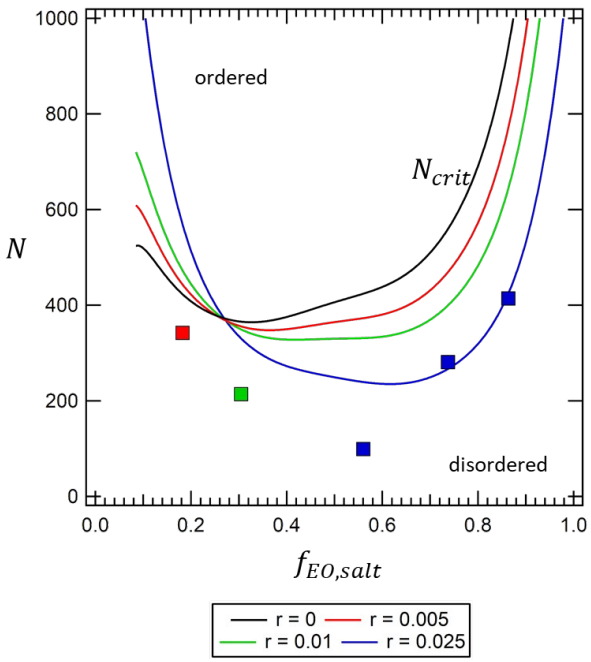

Figure 11: Critical chain length for ordering, N_{crit}, as a function of composition, $f_{EO,salt}$, for SEO/LiTFSI mixtures at 100 °C for different salt concentrations: $r=0$ (black), $r=0.005$ (red), $r=0.01$ (green), and $r=0.025$ (blue). The lines represent the theoretical curves and the squares represent the SEO copolymers discussed in this study. The color of the squares denotes the salt concentration needed to achieve an ordered phase.

We see the emergence of two regimes of salt-dependent phase behavior on either side of $f_{EO,salt}=0.27$, which we refer to as the isotaksis point. At this composition, N_{crit} is independent of salt concentration (all curves for N_{crit} intersect at $f_{EO,salt}=0.27$), i.e., the addition of salt does not affect order in the SEO/LiTFSI mixtures of this composition. We chose the term “isotaksis point” because the word “taksis” means order (spelled τάξις in Greek). At $f_{EO,salt}>0.27$, the addition of salt stabilizes the ordered phases and the order-disorder boundary drops to lower values of N_{crit}. At $f_{EO,salt}<0.27$, the addition of salt stabilizes the disordered phase and the order-disorder boundary moves to higher values of N_{crit}.

The segregation strength in pure block copolymers is characterized by $\Delta(\chi N)$ defined as $\Delta\chi N=\chi N-(\chi N)_{odt}$. At a given temperature and chain length, $\Delta(\chi N)$ is maximum at $f_A = 0.50$. However, this is only valid if χ is independent on composition and chain length. This simplifcation is not valid for SEO/LiTFSI mixtures, and the effect of composition on segregation strength is, perhaps, non-intuitive. We consider copolymers of different compositions at a single chain length and salt concentration. Such systems are represented by a

horizontal line at the chosen value of N in Figure 11. For concreteness, we choose N = 400 and r = 0.025. In Figure 12, we re-plot the $N_{crit}(f_{EO,salt})$ curve for r = 0.025. Note that the salt concentration under these constraints is proportional to the product $r f_{EO,salt}$. The degree of segregation at 100 °C in systems with different $f_{EO,salt}$ can be quantified by $\Delta N = N - N_{crit}$. We show values of ΔN at selected $f_{EO,salt}$ values in Figure 12. Also shown in Figure 12, are schematics that illustrate the degree of segregation at each $f_{EO,salt}$ value. For simplicity, we focus on the compositions of the salt-rich and salt-poor microphases. The salt is assumed to lie in the PEO-rich microphase, but the degree of mixing between the PS and PEO blocks, governed by ΔN, is indicated by the color contrast and interfacial width in each schematic. At $f_{EO,salt}$=0.28(Figure 12a), the SEO/LiTFSI mixture is barely microphase separated as ΔN=42. Here we see a microphase separated morphology with a broad interfacial region. The interface sharpens and the compositional contrast between the microphases increases when $f_{EO,salt}$ is increased to 0.50 (Figure 12b); ΔN=151 at this composition. Increasing $f_{EO,salt}$ further to 0.62 results in the highest degree of segregation possible in systems with N = 400 and r = 0.025 (Figure 12c); ΔN=165 at this composition. This is in contrast with conventional block copolymer melts, where the highest degree of segregation occurs at f_A = 0.50.[14] Finally, at $f_{EO,salt}$=0.84 (Figure 12d), the degree of segregation decreases and ΔN=10. Outside of $0.28 \leq f_{EO,salt} \leq 0.84$, the SEO/LiTFSI mixtures at r=0.025 and N=400 form disordered phases.

Qualtitatively different behavior would be obtained at other values of N and r. It is evident from Figures 11 and 12 that the relationship between segregation strength and copolymer composition in SEO/LiTFSI is complex.

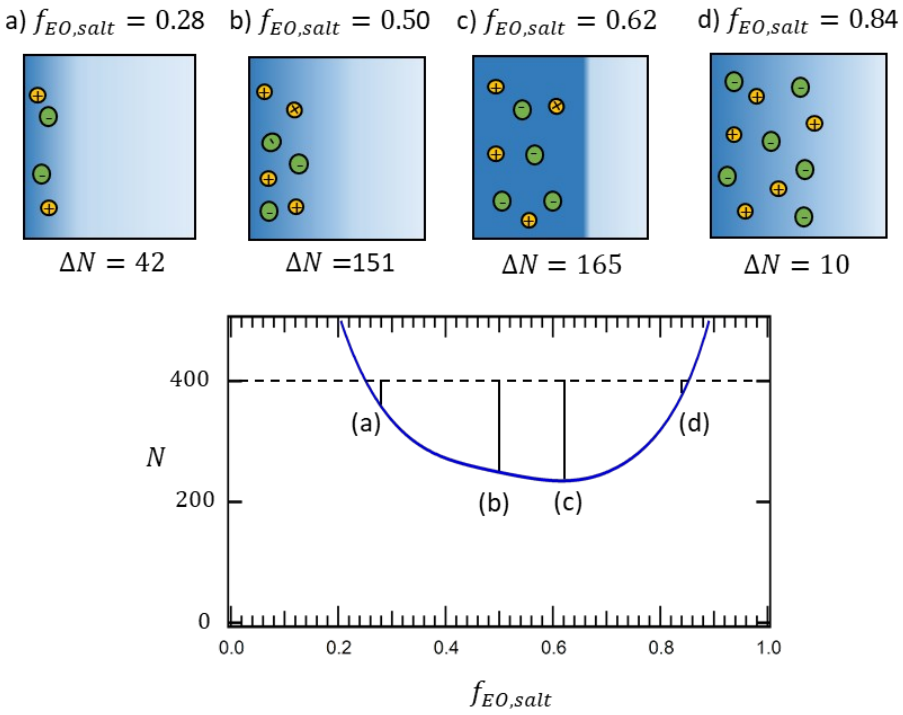

Figure 12: Schematic depicting effect of salt on the degree of segregation, ΔN, of microphase separated of SEO/LiTFSI mixtures with increasing $f_{EO,salt}$ at a constant salt concentration, $r = 0.025$, and total chain length, $N = 400$. The curve represents N_{crit} versus $f_{EO,salt}$ taken from Figure 11. ΔN is defined as the difference between the chosen N and the curve, and the vertical line segments indicate its value at selected values of $f_{EO,salt}$. The salt is assumed to lie in the PEO-rich microphase, but the degree of mixing between the PS and PEO blocks, governed by the magnitude of ΔN, is indicated by the color contrast and interfacial width in each schematic.

MODEL FOR THE ISOTAKSIS POINT

As mentioned in the Introduction, the thermodynamic properties of block copolymer/salt mixtures are complex and governed by many effects including electrostatics, ion solvation, ion-ion and ion-polymer correlations. Constructing a quantitative theory that is consistent with our data is outside the scope of this paper. In fact, the origin of the composition dependence of $\chi_{0,SC}$, the interaction parameter in SEO without salt, is unclear. Nevertheless, it seems important to present a plausible explanation for the existance of the isotaksis composition.

We assume that the ions are distributed uniformly in the disordered state, but they are confined to the PEO microphase in the ordered state, similar in spirit to the original work of Marko and Rabin.[56] If we assume that the salt ions are ideal, then the ion entropy change due to order formation, ΔS_{order}, is given by

$$\Delta S_{order} = n k_B \ln f_{EO} \quad (31)$$

where n is the number of independent ions and k_B is the Boltzmann constant. For simplicity we ignore the difference between f_{EO} and $f_{EO,salt}$ in this analysis which is a reasonable approximation for $r \leq 0.025$, the range of salt concentrations covered in Figure 11. If we assume a lattice model wherein n_t is the total number of lattice sites, n_{EO} is the number of lattice sites occupied by EO and each lattice site is either occupied by a polymer segment or a salt ion, then

$$\frac{\Delta S_{order}}{n_t k_B} = r \frac{n_{EO}}{n_t} \ln(f_{EO}) = r f_{EO} \ln(f_{EO}) \quad (32)$$

Note that the entropic contribution is a linear function of r.

We assume that this tendency to disorder is balanced by the solvation energy[33,34] that induces ordering, and is quantified by Equation 4. We thus define a theoretical χ, χ_{th}, that is the sum of the two contributions:

$$\chi_{th} = \chi_0 + m_n r + \frac{r f_{EO} \ln(f_{EO})}{f_{EO}(1 - f_{EO})} \quad (33)$$

where m_n is a nominal value of m that is assumed to be independent of composition. In many previous studies on mixtures of salt and SEO copolymers[35,51,55], m_n has been shown to be about 1.7. At the isotaksis point ($f_{EO,it} = 0.31$),

$$\frac{d\chi_{th}}{dr} = 0 = m_n + \frac{f_{EO,it} \ln(f_{EO,it})}{f_{EO,it}(1 - f_{EO,it})} \quad (34)$$

and

$$m_n = \frac{-f_{EO,it} \ln(f_{EO,it})}{f_{EO,it}(1 - f_{EO,it})} \quad (35)$$

For a system with $m_n = 1.7$, the isotakis point according to Equation 35 is predicted to occur at $f_{EO} = 0.31$. The experimentally measured isotaksis composition is 0.27. The quantitative agreement between experiments and the model is probably fortuitious, as the model is highly simplified. For

example, one could envision placing a prefactor of 2 on the right hand side of Equation 32 to account for salt dissociation. However, the extent to which positively and negatively charged ions are independent in low dielectric media like PEO remains unclear. In addition to this, a complete theory for the isotaksis composition would require inclusion of electrostatic interactions, ion correlations, and physical crosslinking due to interactions between ions and polymer backbones.

CONCLUSIONS

We have characterized thermodynamics of SEO/LiTFSI mixtures by analyzing SAXS scattering patterns from disordered systems. RPA was used to determine χ_{SC}, as a function of block copolymer composition, chain length, temperature and salt concentration. In the neat copolymers, $\chi_{0,SC}$ is a linear function of $\left(Nf_{EO}\right)^{-1}$. At a given temperature, block copolymer composition and chain length, $\chi_{eff,SC}$ increases linearly with added salt. The data are only weak functions of temperature as shown in Figures 4 and 6, and therefore these conclusions apply across the entire temperature window studied ($75<T\left(°C\right)<130$). The framework of Sanchez[15] was used to determine χ_{eff} from $\chi_{eff,SC}$ in both salty and salt-free systems. We use the term χ_{eff} as it represents interactions between PEO/LiTFSI and PS. SCFT results on pure block copolymers[11] are used to determine the relationship between $\chi_{eff}N$ and

composition, $f_{EO,salt}$, at the order-disorder transition. We refer to the value of N at the order-disorder transition as N_{crit}. All of the SEO copolymers used in this study were disordered in the neat state and order upon salt addition. This enables a direct comparison between experimentally determined values of N_{crit} with theoretical predictions. At $f_{EO,salt}$values greater than 0.27, the addition of salt decreases N_{crit}, i.e., the ordered phase is stabilized. At $f_{EO,salt}$ values less than 0.27, the addition of salt increases N_{crit}, i.e., the disordered phase is stabilized. We propose calling $f_{EO,salt} = 0.27$ the isotaksis point. A simple theoretical model is proposed to predict the existence of this point. The use of χ to describe the phase behavior of neat block copolymers is strictly valid in the limit of infinite chain length. Fluctuation effects become important at finite chain lengths and this leads to non-trivial changes in phase behavior.[50,57,58] Strictly speaking, the implication of the isotaksis point is that the phase behavior of SEO/LiTFSI mixtures at this composition should be independent of salt concentration. Instead, experiments show anamalous phase behavior in the vicinity of this composition. In particular the addition of salt to a disordered phase in the vicinity of the isotaksis point gives rise to two coexisting body centered cubic lattices which then disorder before finally ordering into the expected hexagonnally packed cylinder morphology.[59] While further work is required to determine the underpinnings of such observations, the present framework provides a platform to do so.

AUTHOR INFORMATION

Corresponding Author

*(NPB) E-mail: nbalsara@berkeley.edu

Author Contributions:

The manuscript was written through contributions of all authors. All authors have given approval to the final version of the manuscript.

Notes:

The authors declare no competing financial interest.

ACKNOWLEDGEMENTS

Primary funding for this work was provided by the National Science Foundation through Award DMR-1505444. Work at the Advanced Light Source, which is a DOE Office of Science User Facility, was supported by Contract No. DE-AC02-05CH11231. Work at the Stanford Synchrotron Radiation Light Source, a user facility at SLAC National Accelerator Laboratory, was supported by the U.S. Department of Energy, Office of Science, Office of Basic Energy Sciences under Contract No. DE-AC02-76SF00515. W.S.L. acknowledges funding from the National Science Foundation Graduate Student Research Fellowship DGE-1106400. We thank the reviewers for their feedback to help improve the manuscript.

SUPPORTING INFORMATION

Additional information on the salt concentration and temperature dependence of the chain-stretching parameter, α, for the SEO/LiTFSI mixtures presented in the main text.

LIST OF SYMBOLS

a_i	statistical segment length of species i (nm)
b_i	X-ray scattering length of species i (nm mer^{-1})
B_i	scattering length density of species i (nm^{-2} mer^{-1})
C_i	Self consistent field theory fitting parameters
C	electron density contrast (cm^{-1})
d	domain size (nm)
f_A	volume fraction of species A
f_{EO}	volume fraction of PEO block
$I(q)$	scattering intensity (cm^{-1})
$I_{dis}(q)$	disordered copolymer scattering intensity (cm^{-1})

k_B	Boltzmann constant
m	proportionality constant
m_{it}	proportionality constant at isotaksis composition
M_i	number-averaged molecular weight of species *i* (kg mol^{-1})
N_i	number-averaged degree of polymerization of species *i* (sites chain^{-1})
N_A	Avogadro's number
N_{crit}	critical chain length for ordering
n	number of independent ions
n_{EO}	number of EO sites
n_t	total number of lattice sites
q	scattering vector (nm^{-1})
q^*	primary peak of scattering vector (nm^{-1})
r	salt concentration ([Li$^+$] [EO]$^{-1}$)
$R_{g,i}$	radius of gyration of species *i* (nm)
$S(q)$	scattering structure factor
T	temperature (K)
Y_{LiTFSI}	volume fraction of salt in PEO/LiTFSI microphase

Greek

α	chain-stretching parameter
ΔS_{order}	change in entropy due to ordering
ΔN	degree of segregation
ϵ	conformational asymmetry parameter
χ	Flory-Huggins interaction parameter
χ_{SC}	Flory-Huggins interaction parameter from scattering
χ_0	Flory-Huggins interaction parameter of salt free system
χ_{th}	theoretical Flory-Huggins interaction parameter
χ_{eff}	effective Flory-Huggins interaction parameter
χN	segregation strength
$(\chi N)_{odt}$	segregation strength at the ODT
ν_i	molar volume of species *i* (cm^3 mol^{-1})
ν_{ref}	reference volume (nm^3 site^{-1})
ρ_i	density of species *i* (g cm^{-3})

LIST OF ABBREVIATIONS

EO	ethylene oxide

LiTFSI	lithium bis(trifluoromethanesulfonyl) imide salt
N_A	Avogadro's number
ODT	order-disorder transition
PEO	poly(ethylene oxide)
PS	polystyrene
RPA	Random Phase Approximation
S	styrene
SAXS	small angle X-ray scattering
SCFT	Self-Consistent Field Theory
SEO	polystyrene-*block*-poly(ethylene oxide)

REFERENCES

(1) Mizushima, K.; Jones, P. C.; Wiseman, P. J.; Goodenough, J. B. LixCoO 2 (0<x<1): A New Cathode Material for Batteries of High Energy Density. *Mat. Res. Bull* **1980**, *15* (6), 783–789.

(2) Hallinan, D. T.; Balsara, N. P. Polymer Electrolytes. *Annu. Rev. Mater. Res* **2013**, *43*, 503–525.

(3) Young, W. S.; Kuan, W. F.; Epps, T. H. Block Copolymer Electrolytes for Rechargeable Lithium Batteries. *J. Polym. Sci. Part B Polym. Phys.* **2014**, *52* (1), 1–16.

(4) Morris, M. A.; An, H.; Lutkenhaus, J. L.; Epps, T. H. Harnessing the Power of Plastics: Nanostructured Polymer Systems in Lithium-Ion Batteries. *ACS Energy Letters*. **2017,** *2* (8), 1919–1936.

(5) Soo, P. P.; Huang, B.; Jang, Y.-I.; Chiang, Y.-M.; Sadoway, D. R.; Mayes, A. M. Rubbery Block Copolymer Electrolytes for Solid-State Rechargeable Lithium Batteries. *J. Electrochem. Soc*. **1999**, *146* (1), 32–37.

(6) Miller, T. F.; Wang, Z. G.; Coates, G. W.; Balsara, N. P. Designing Polymer Electrolytes for Safe and High Capacity Rechargeable Lithium Batteries. *Accounts of Chemical Research*. **2017**, *50* (3), 590–593.

(7) Glynos, E.; Petropoulou, P.; Mygiakis, E.; Nega, A. D.; Pan, W.; Papoutsakis, L.; Giannelis, E. P.; Sakellariou, G.; Anastasiadis, S. H. Leveraging Molecular Architecture To Design New, All-Polymer Solid Electrolytes with Simultaneous Enhancement in Modulus and Ionic Conductivity. *Macromolecules* **2018**, *51* (7), 2542–2550.

(8) Pesko, D. M.; Timachova, K.; Bhattacharya, R.; Smith, M. C.; Villaluenga, I.; Newman, J.; Balsara, N. P. Negative Transference Numbers in Poly(Ethylene Oxide)-Based Electrolytes. *J. Electrochem. Soc*. **2017**, *164* (11), E3569–E3575.

(9) Singh, M.; Odusanya, O.; Wilmes, G. M.; Eitouni, H. B.; Gomez, E. D.; Patel, a J.; Chen, V. L.; Park, M. J.; Fragouli, P.; Iatrou, H.; Hadjichristidis, N.; Cookson, D.; Balsara, N. P. Effect of Molecular Weight on the Mechanical and Electrical Properties of Block Copolymer Electrolytes. *Macromolecules* **2007**, *40* (13), 4578–4585.

(10) Bates, F. S.; Fredrickson, G. H. Block Copolymer Thermodynamics: Theory and Experiment. *Annu. Rev. Phys. Chem*. **1990,** *41* (1), 525–557.

(11) Cochran, E. W.; Garcia-Cervera, C. J.; Fredrickson, G. H. Stability of the Gyroid Phase in Diblock Copolymers at Strong Segregation. *Macromolecules* **2006**, *39* (7), 2449–2451.

(12) Knychała, P.; Timachova, K.; Banaszak, M.; Balsara, N. P. 50th Anniversary Perspective: Phase Behavior of Polymer Solutions and Blends. *Macromolecules* **2017**, *50* (8), 3051–3065.

(13) Matsen, M. W.; Schick, M. Stable and Unstable Phases of a Diblock Copolymer Melt. *Phys. Rev. Lett.* **1994,** *72* (16), 2660–2663.

(14) Leibler, L. Theory of Microphase Separation in Block Copolymers. *Macromolecules* **1980**, *13* (10), 1602–1617.

(15) Sanchez, I. C. Relationships between Polymer Interaction Parameters. *Polymer* **1989**, *30* (3), 471–475.

(16) de Gennes, P. G. Scaling Concepts in Polymer Chemsitry; Cornell University Press: Ithaca, NY, 1979.

(17) Bates, F. S.; Muthukumar, M.; Wignall, G. D.; Fetters, L. J. Thermodynamics of Isotopic Polymer Mixtures: Significance of Local Structural Symmetry. *J. Chem. Phys.* **1988**, *89* (1), 535–544.

(18) Wanakule, N. S.; Lai, P.; Robertson, M. L.; Balsara, N. P.; Nedoma, A. J.; Jackson, A. Phase Diagrams of Blends of Polyisobutylene and Deuterated Polybutadiene as a Function of Chain Length. *Macromolecules* **2011**, *44* (8), 3077–3084.

(19) Ellison, C. J.; Meuler, A. J.; Qin, J.; Evans, C. M.; Wolf, L. M.; Bates, F. S. Bicontinuous Polymeric Microemulsions from Polydisperse Diblock Copolymers. *J. Phys. Chem. B* **2009**, *113* (12), 3726–3737.

(20) Meuler, A. J.; Ellison, C. J.; Qin, J.; Evans, C. M.; Hillmyer, M. A.; Bates, F. S. Polydispersity Effects in Poly(Isoprene-b-Styrene-b-Ethylene Oxide) Triblock Terpolymers. *J. Chem. Phys.* **2009**, *130* (23), 234903.

(21) Sing, C. E.; Zwanikken, J. W.; de la Cruz, M. O. Electrostatic Control of Block Copolymer Morphology. *Nat. Mater*. **2014**, *13*, 694–698.

(22) Sing, C. E.; Zwanikken, J. W.; De La Cruz, M. O. Theory of Melt Polyelectrolyte Blends and Block Copolymers: Phase Behavior, Surface Tension, and Microphase Periodicity. *J. Chem. Phys*. **2015**, *142* (3), 1–18.

(23) Pryamitsyn, V. A.; Kwon, H.-K.; Zwanikken, J. W.; Olvera de la Cruz, M. Anomalous Phase Behavior of Ionic Polymer Blends and Ionic Copolymers. *Macromolecules* **2017**, *50* (13), 5194–5207.

(24) Brown, J. R.; Seo, Y.; Hall, L. M.; Lowrie, W. G. Ion Correlation Effects in Salt-Doped Block Copolymers. *Phys. Rev. Lett.* **2018**, *120* (12), 1–7.

(25) Nakamura, I. Ion Solvation in Polymer Blends and Block Copolymer Melts: Effects of Chain Length and Connectivity on the Reorganization of Dipoles. *J. Phys. Chem. B* **2014**, *118* (21), 5787–5796.

(26) Liu, L.; Nakamura, I. Solvation Energy of Ions in Polymers: Effects of Chain Length and Connectivity on Saturated Dipoles near Ions. *J. Phys. Chem. B* **2017**, *121* (14), 3142–3150.

(27) Nakamura, I. Effects of Dielectric Inhomogeneity and Electrostatic Correlation on the Solvation Energy of Ions in Liquids. *J. Phys. Chem. B* **2018**, *122* (22), 6064-6071.

(28) Ren, C. L.; Nakamura, I.; Wang, Z. G. Effects of Ion-Induced Cross-Linking on the Phase Behavior in Salt-Doped Polymer Blends. *Macromolecules* **2016**, *49* (1), 425–431.

(29) Hou, K. J.; Qin, J. Solvation and Entropic Regimes in Ion-Containing Block Copolymers. *Macromolecules* **2018**, *51* (19), 7463–7475.

(30) Wang, Z. G. Effects of Ion Solvation on the Miscibility of Binary Polymer Blends. *J. Phys. Chem. B* **2008**, *112* (50), 16205–16213.

(31) Nakamura, I.; Wang, Z.-G. Salt-Doped Block Copolymers: Ion Distribution, Domain Spacing and Effective χ Parameter. *Soft Matter* **2012**, *8* (36), 9356.

(32) Nakamura, I.; Wang, Z. G. Thermodynamics of Salt-Doped Block Copolymers. *ACS Macro Lett.* **2014**, *3* (8), 708–711.

(33) Nakamura, I.; Balsara, N. P.; Wang, Z. G. Thermodynamics of Ion-Containing Polymer Blends and Block Copolymers. *Phys. Rev. Lett.* **2011**, *107* (19), 1–5.

(34) Ruzette, G.; Soo, P. P.; Sadoway, D. R.; Mayes, A. M. Melt-Formable Block Copolymer Electrolytes for Lithium Rechargeable Batteries. *J. Electrochem. Soc.* **2001**, *148* (6), A537–A543.

(35) Loo, W. S.; Galluzzo, M. D.; Li, X.; Maslyn, J. A.; Oh, H. J.; Mongcopa, K. I.; Zhu, C.; Wang, A. A.; Wang, X.; Garetz, B. A.; Balsara, N. P. Phase Behavior of Mixtures of Block Copolymers and a Lithium Salt. *J. Phys. Chem. B* **2018**, *122* (33), 8065–8074.

(36) Hadjichristidis, N.; Iatrou, H.; Pispas, S.; Pitsikalis, M. Anionic Polymerization: High Vacuum Techniques. *J. Polym. Sci. Part A Polym. Chem.* **2000**, *38* (18), 3211–3234.

(37) Teran, A. a.; Balsara, N. P. Thermodynamics of Block Copolymers with and without Salt. *J. Phys. Chem. B* **2014**, *118* (1), 4–17.

(38) Thelen, J. L.; Wang, A. A.; Chen, X. C.; Jiang, X.; Schaible, E.; Balsara, N. P. Correlations between Salt-Induced Crystallization, Morphology, Segmental Dynamics, and Conductivity in Amorphous Block Copolymer Electrolytes. *Macromolecules* **2018**, *51* (5), 1733–1740

(39) Gilbert, J. B.; Luo, M.; Shelton, C. K.; Rubner, M. F.; Cohen, R. E.; Epps, T. H. Determination of Lithium-Ion Distributions in Nanostructured Block Polymer Electrolyte Thin Films by X-Ray Photoelectron Spectroscopy Depth Profiling. *ACS Nano* **2015**, *9* (1), 512–520.

(40) Gartner, T. E.; Morris, M. A.; Shelton, C. K.; Dura, J. A.; Epps, T. H. Quantifying Lithium Salt and Polymer Density Distributions in Nanostructured Ion-Conducting Block Polymers. *Macromolecules* **2018**, *51* (5), 1917–1926.

(41) Gomez, E. D.; Panday, A.; Feng, E. H.; Chen, V.; Stone, G. M.; Minor, A. M.; Kisielowski, C.; Downing, K. H.; Borodin, O.; Smith, G. D.; Balsara, N. P. Effect of Ion Distribution on Conductivity of Block Copolymer Electrolytes. *Nano Lett.* **2009**, *9* (3), 1212–1216.

(42) Hexemer, A.; Bras, W.; Glossinger, J.; Schaible, E.; Gann, E.; Kirian, R.; MacDowell, A.; Church, M.; Rude, B.; Padmore, H. A SAXS/WAXS/GISAXS Beamline with Multilayer Monochromator. In *Journal of Physics: Conference Series*; 2010; Vol. 247, pp 1–11.

(43) Ilavsky, J. Nika: Software for Two-Dimensional Data Reduction. *J. Appl. Crystallogr.* **2012**, *45* (2), 324–328.

(44) Matsen, M. W.; Bates, F. S. Conformationally Asymmetric Block Copolymers. *J. Polym. Sci. Part B Polym. Phys*. **1997**, *35* (6), 945–952.

(45) Eitouni, H. B.; Balsara, N. P. CHAPTER 19 Thermodynamics of Polymer Blends. *Phys. Prop. Polym. Handb*. *2e* **2006**, 339–356.

(46) Irwin, M. T.; Hickey, R. J.; Xie, S.; Bates, F. S.; Lodge, T. P. Lithium Salt-Induced Microstructure and Ordering in Diblock Copolymer/Homopolymer Blends. *Macromolecules* **2016**, *49* (13), 4839–4849.

(47) Zhang, W.; Huang, M.; Abdullatif, S. al; Chen, M.; Shao-Horn, Y.; Johnson, J. A. Reduction of (Meth)Acrylate-Based Block Copolymers Provides Access to Self-Assembled Materials with Ultrasmall Domains. *Macromolecules* **2018**, *51* (17), 6757–6763.

(48) Thelen, J. L.; Inceoglu, S.; Venkatesan, N. R.; Mackay, N. G.; Balsara, N. P. Relationship between Ion Dissociation, Melt Morphology, and Electrochemical Performance of Lithium and Magnesium Single-Ion Conducting Block Copolymers. *Macromolecules* **2016**, *49* (23), 9139–9147

(49) Jung, H. Y.; Kim, S. Y.; Kim, O.; Park, M. J. Effect of the Protogenic Group on the Phase Behavior and Ion Transport Properties of Acid-Bearing Block Copolymers. *Macromolecules* **2015**, *48* (17), 6142–6152.

(50) Fredrickson, G. H.; Helfand, E. Fluctuation Effects in the Theory of Microphase Separation in Block Copolymers. *J. Chem. Phys.* **1987**, *87* (1), 697–705.

(51) Wanakule, N. S.; Virgili, J. M.; Teran, A. A.; Wang, Z. G.; Balsara, N. P. Thermodynamic Properties of Block Copolymer Electrolytes Containing Imidazolium and Lithium Salts. *Macromolecules* **2010**, *43* (19), 8282–8289.

(52) Young, W.; Epps, T. H. Salt Doping in PEO-Containing Block Copolymers: Counterion and Concentration Effects. *Macromolecules* **2009**, *42 (*7), 2672–2678.

(53) Gunkel, I.; Thurn-Albrecht, T. Thermodynamic and Structural Changes in Ion-Containing Symmetric Diblock Copolymers: A Small-Angle X-Ray Scattering Study. *Macromolecules* **2012**, *45* (1), 283–291.

(54) Zardalidis, G.; Ioannou, E. F.; Gatsouli, K. D.; Pispas, S.; Kamitsos, E. I.; Floudas, G. Ionic Conductivity and Self-Assembly in Poly(Isoprene- b -Ethylene Oxide) Electrolytes Doped with LiTf and EMITf. *Macromolecules* **2015**, *48* (5), 1473–1482

(55) Loo, W. S.; Balsara, N. P. Organizing Thermodynamic Data Obtained from Multicomponent Polymer Electrolytes: Salt-Containing Polymer Blends and Block Copolymers. *J. Polym. Sci. Part B Polym. Phys.* **2019**, 1–11. DOI: 10.1002/polb.24800.

(56) Marko, J.; Rabin, Y. Microphase Separation of Charged Diblock Copolymers: Melts and Solutions. *Macromolecules* **1992**, *25*, 1503–1509.

(57) Medapuram, P.; Glaser, J.; Morse, D. C. Universal Phenomenology of Symmetric Diblock Copolymers near the Order-Disorder Transition. *Macromolecules* **2015**, *48* (3), 819–839.

(58) Grzywacz, P.; Qin, J.; Morse, D. C. Renormalization of the One-Loop Theory of Fluctuations in Polymer Blends and Diblock Copolymer Melts. *Phys. Rev. E - Stat. Nonlinear, Soft Matter Phys*. **2007**, *76* (6), 1–33.

(59) Loo, W. S.; Jiang, X.; Maslyn, J. A.; Oh, H. J.; Zhu, C.; Downing, K. H.; Balsara, N. P. Reentrant Phase Behavior and Coexistence in Asymmetric Block Copolymer Electrolytes. *Soft Matter* **2018**, *14* (15), 2789–2795.